Corrosion Inhibition by *Isertia coccinea* Plant Extract in Hydrochloric Acid Solution

M. Lebrini, F. Robert[*]*, P.A. Blandinières, C. Roos*

Laboratoire Matériaux et Molécules en Milieu Amazonien, UAG-UMR ECOFOG,
Campus Trou Biran, Cayenne 97337, French Guiana.
[*]E-mail: florent.robert@guyane.univ-ag.fr

The effect of alkaloids extracted from *Isertia coccinea* plant (AEIC) on the corrosion of C38 steel in 1 M hydrochloric acid was investigated by electrochemical impedance spectroscopy (EIS) and potentiodynamic polarization techniques. Potentiodynamic polarization curves indicated that the extract behave as mixed-type inhibitor. The experimental data obtained from EIS method show a frequency distribution and therefore a modelling element with frequency dispersion behaviour, a constant phase element (CPE) has been used. The inhibition efficiencies of the extract calculated by three methods show the same tendency. Inhibition was found to increase with increasing concentration of the plant extract. The results obtained show that the extract solution of the plant could serve as an effective inhibitor for the corrosion of C38 steel in hydrochloric acid solution. The apparent activation energy of the process taking place in inhibitor presence was determined on the ground of four temperature values in the range from 25 °C to 55 °C using the data obtained by two independent methods. Theoretical fitting of different isotherms, Langmuir, Temkin and Frunkin, were tested to clarify the nature of adsorption.

1. INTRODUCTION

Iron and steel, the most commonly used metals; corrode in many media including most outdoor atmospheres. A survey of literature reveals that the applicability of organic compounds as corrosion inhibitors for mild steel in acidic media has been recognized for a long time [1–7]. A large number of organic compounds, particularly those containing nitrogen, oxygen or sulphur in a conjugated system, are known to be applied as inhibitors to control acid corrosion of iron and steel. Some investigations have in recent times been made into the corrosion inhibiting properties of natural products of plant origin, and have been found to generally exhibit good inhibition efficiencies [8–20]. The significance

of this area of research is primarily due to the fact that natural products are environmentally friendly and ecologically acceptable. The yield of these natural products as well as the corrosion inhibition abilities of the plant extracts vary widely depending on the part of the plant [21–22] and its location [23]. Of importance also is the specificity of corrosion inhibiting compounds. One compound effective in a certain medium with a given metal may be ineffective for the same metal in another medium [24]. The inhibitive effect of some plants solution extract is due to the adsorption of molecules of phytochemicals present in the plant on the surface of the metal, which blocks the metal surface and thus does not permit the corrosion process to take place. Our research group has recently reported on the corrosion inhibitive effectiveness of C38 steel by *Oxandra asbeckii* [12], *Annona squamosa* [11], *Simira tinctoria, Guatteria ouregou* [25], and the latest on *Palicourea guianensis* [13]. All alkaloids extracted from these plants acted as good corrosion inhibitors for C38 steel in 1 M HCl medium. The present report continues to focus on the broadening application of plant extracts for metallic corrosion control and reports on the inhibiting effect of the alkaloids extract from *Isertia coccinea* plant (AEIC) on C38 steel corrosion in acidic solution. Also, the effect of temperature on the values of the electrochemical parameters characterizing the system has been recorded by polarisation curves and electrochemical impedance spectroscopy.

2. EXPERIMENTAL

2.1. Electrode and solution

Corrosion tests have been carried out on electrodes cut from sheets of C38 steel. Steel strips containing 0.36 wt% C, 0.66 wt% Mn, 0.27 wt% Si, 0.02 wt% S, 0.015 wt% P, 0.21 wt% Cr, 0.02 wt% Mo, 0.22 wt% Cu, 0.06 wt% Al and the remainder iron. The specimens were embedded in epoxy resin leaving a working area of 0.78 cm^2. The working surface was subsequently ground with 180 and 1200 grit grinding papers, cleaned by distilled water and ethanol. The solutions (1 M HCl) were prepared by dilution of an analytical reagent grade 33% HCl with doubly distilled water. All the tests were performed at ambient temperature (25 °C).

2.2. Preparation of plant extract

Extraction ─ The procedure adopted for the alkaloids extraction method was the same as described elsewhere [26]. After collecting alkaloids extract, the remaining extract was analyzed by HPLC (Fig. 1). It contains over 9 major peaks along with many small peaks indicating presence of more than 30 compounds. The small peaks may be attributed to the compounds present in small quantities as well as disintegrated major compounds. Since retention time of compounds is close to each other and it is very difficult to separate them, hence the total alkaloids extract from *Isertia coccinea* plant was used as such for corrosion inhibition studies. The concentration range of alkaloids extract from *Isertia coccinea* plant employed was 5 – 100 mg L^{-1}.

HPLC system ─ The HPLC separations were performed on a Supelco Discovery HS PEG column (25 cm x 21.2 mm, 5 lm) using a Waters system equipped with a W600 pump and a W2996 photodiode array absorbance detector. The samples were injected manually through a Rheodyne injector and the flow rate was 1 ml/min.
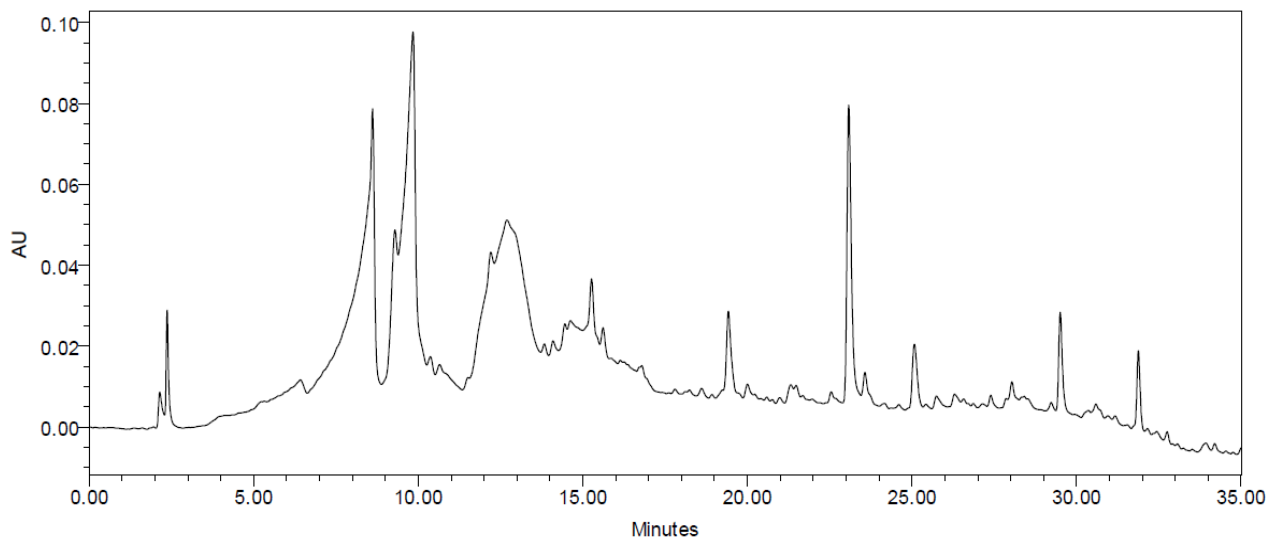

Figure 1. HPLC spectroscopy spectra of total alkaloid extract from *Isertia coccinea.*

2.3. Electrochemical measurements

Electrochemical measurements, including potentiodynamic polarization curves and electrochemical impedance spectroscopy (EIS) were performed in a three-electrode cell. The C38 steel specimen was used as the working electrode, a platinum wire as the counter electrode and a saturated calomel electrode (SCE) as the reference electrode. Before each Tafel and EIS experiments, the electrode was allowed to corrode freely and its open-circuit potential (OCP) was recorded as a function of time during 3 h, the time necessary to reach a quasi-stationary value for the open-circuit potential. This steady-state OCP corresponds to the corrosion potential (E_{corr}) of the working electrode. The procedure adopted for the electrochimical measurements was the same as described elsewhere [11,12]. The Tafel and EIS data were analysed using graphing and analyzing impedance software, version EC-Lab V9.97.

3. RESULTS AND DISCUSSION

3.1. Polarisation curves

Fig. 2 shows a typical record of Tafel polarization measurements for C38 steel in 1 M HCl in the absence and presence of the AEIC at 25 °C. From the figure, it can be seen that addition of the extract

to acid media affected both the cathodic and anodic parts of the curves. Hence, the addition of AEIC to HCl solution reduces the anodic dissolution of iron and also retards the cathodic hydrogen evolution reaction. Therefore, the cathodic currents remain almost unchanged with increasing the concentration of the extract. Table 1 lists the polarization parameters for corrosion of C38 steel in the presence of different concentrations of the investigated extract. The polarization resistances (R_p) were calculated from the linear *I-E* plots in the potential range ±25 mV from the corrosion potential. The R_p fit was obtained with a good correlation coefficient ($R^2 \geq 0.999$). The corresponding R_P values are also given in Table 1. It is found (Table 1) that, the corrosion current density shows a marked tendency to decrease with concentration and its values are much lower than in the uninhibited acidic solutions. Whereas the polarization resistances values tend to increase upon addition of extract. Corrosion potential shifted to negative and positive direction; although there was not a specific relation between E_{corr} and extract concentration. Since the largest displacement exhibited by extract is 6 and 32 mV cathodically and anodically compared to the blank, respectively. This negative and positive shift indicates that AEIC behave as mixed-type inhibitors. *IE*(%) increased with inhibitor concentration reaching a maximum value at 100 mg L^{-1}. The inhibition efficiencies calculated from R_p results show the same trend as those obtained from I_{corr}.
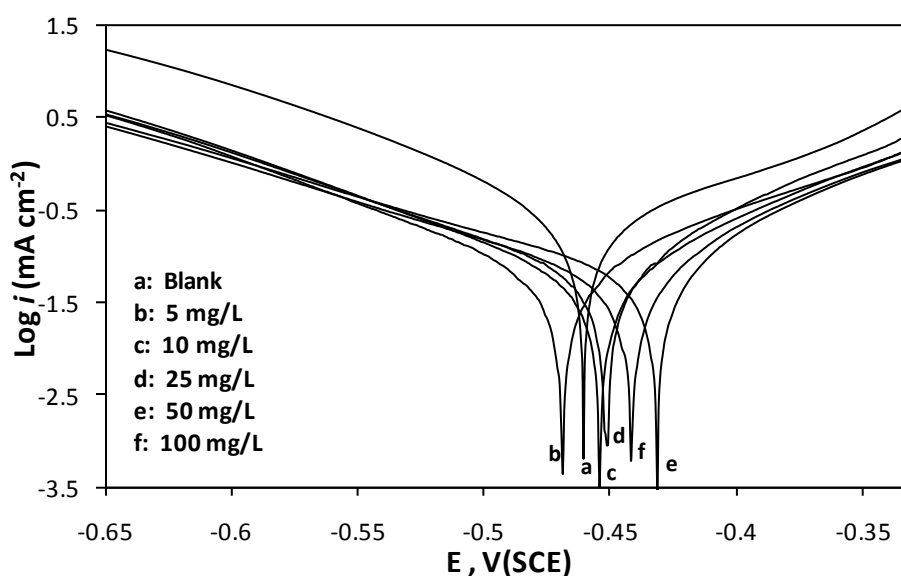

Figure 2. Polarisation curves for C38 steel in 1 M HCl containing different concentrations of AEIC.

3.2. Electrochemical impedance spectroscopy (EIS)

The impedance plots for C38 in 1 M HCl solutions containing different concentrations of AEIC are shown in Figs. 3 and 4. All EIS spectra show mainly one semicircle in Nyquist plots and one time-constant feature in Bode plots, which represents the resistive and capacitive properties of the metal–solution interface. Inspections of the data reveal that the addition of inhibitors results in an increase in the diameter of the semicircular capacitive loop (Fig. 3), in the impedance of the double layer (Fig. 4a,

representative example) and in the maximum phase angle (Fig. 4b, representative example). Focusing on the main feature of the EIS spectra, the simple equivalent electrical circuit shown in Fig. 5, can be satisfactorily used for spectra fitting, where R_s is the solution resistance between the reference electrode and working electrode, R_{ct} is the charge transfer resistance, and CPE is a constant phase element that often is used instead of a double layer capacitance to account for the non-ideal capacitive response from the interface [27]. The fit parameter, exponential factor n, is often related to the degree of heterogeneity of the interface and/or surface film. A good fit was obtained with our experimental data, as shown in Fig. 4a and b (representative examples) where the points represent experimental data and the solid lines are spectra simulations based on the proposed electrical equivalent circuit.

Table 1. Polarization parameters and the corresponding inhibition efficiency for the corrosion of C38 steel in 1 M HCl containing different concentrations of AEIC at 25 °C.

Concentration mg L^{-1}	E$_{corr}$ vs SCE	I$_{corr}$	β$_c$	β$_a$	R$_p$	IE Icorr	IE Rp
	(mV)	(μA cm^{-2})	(mV dec^{-1})	(mV dec^{-1})	(Ω cm^2)	(%)	(%)
1 M HCl	-463	232	89	106	76	—	—
AEIC							
5	-469	72	72	103	228	69	67
10	-455	54	78	102	298	77	74
25	-450	52	73	114	310	78	75
50	-431	47	71	126	318	80	76
100	-443	45	78	122	348	81	78

The main parameters deduced from the fit of Nyquist diagram for 1 M HCl medium containing various concentrations of AEIC are given in Table 2. In the same Table are shown also the calculated ˝double layer capacitance˝ values (C_{dl}), using the Eq. (1) [28–30] and the relaxation time constants using the Eq. (2) [31,32].

$$C_{dl} = (A.R_{ct}^{\,1-n})^{1/n} \tag{1}$$

$$\tau = C_{dl}\, R_{ct} \tag{2}$$

Where A is the CPE constant and n is a CPE exponent. It's found that, the R_{ct} values increased with the increase of the concentration of inhibitor, which shows protection of C38 surface by the inhibitor.

Whereas the values of C_{dl} decreased with the increase in the concentration of inhibitor, which is due to the increase in the thickness of protective layer at higher concentrations and therefore suggests that extract functions by adsorption at the steel–solution interface. Also, the value of the proportional factor *A* of CPE decreased with the increase in the concentration. The values of *n* increased with the increase of the concentration of inhibitor, which shows a reduction of surface inhomogeneity due to the adsorption of inhibitor molecules on the most active adsorption sites at the C38 steel surface. The time constants τ, calculated using the Eq. (2), shows a marked tendency to increase with concentration and its values are much higher than in the uninhibited acidic solution which means slow adsorption process. The inhibition efficiencies (*IE*) are calculated as follows

$$IE\,(\%) = [(R_{ct} - R_{ct}^{0})/R_{ct}] \times 100 \qquad (3)$$

Inhibition efficiency as a function of concentrations of extract at 25 °C is plotted in Fig.6. In the three cases, it can be observed, from this figure that the protection efficiency increases with increasing the concentration of extract and inhibits the corrosion of steel in 1 M HCl solution. Maximum of inhibition efficiency was achieved at 100 mg/L of the extract and a further increase in concentration did not cause any appreciable change in the performance of the inhibitor. The results of electrochemical studies (impedance and polarization measurements) were in good agreement with slight deviations.
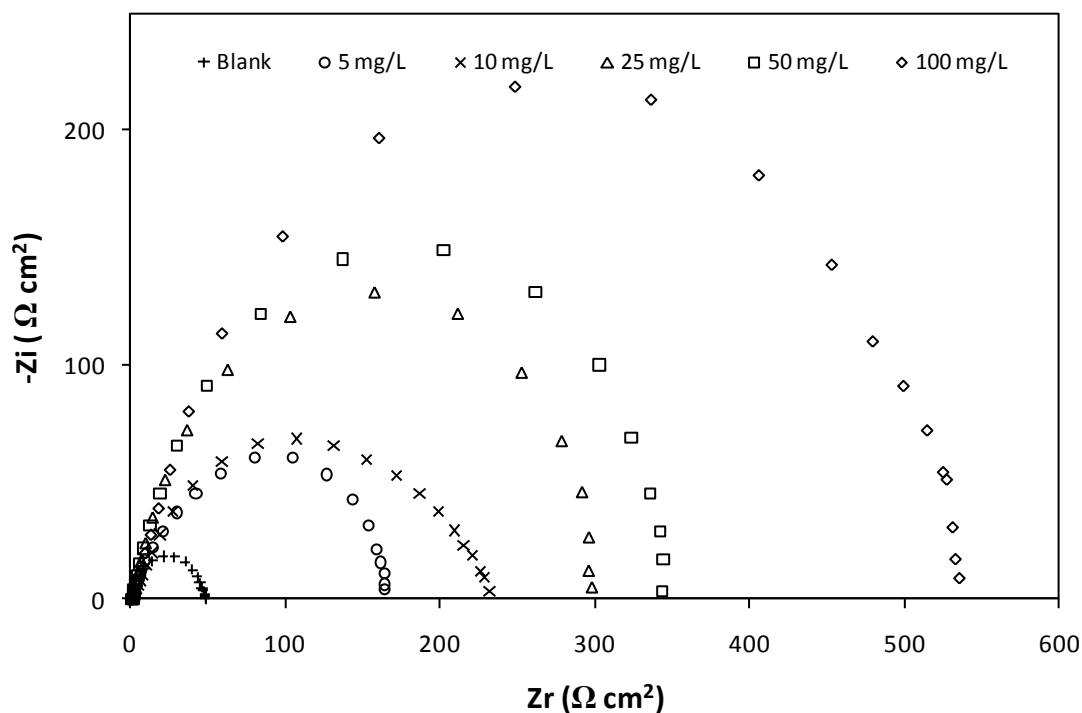

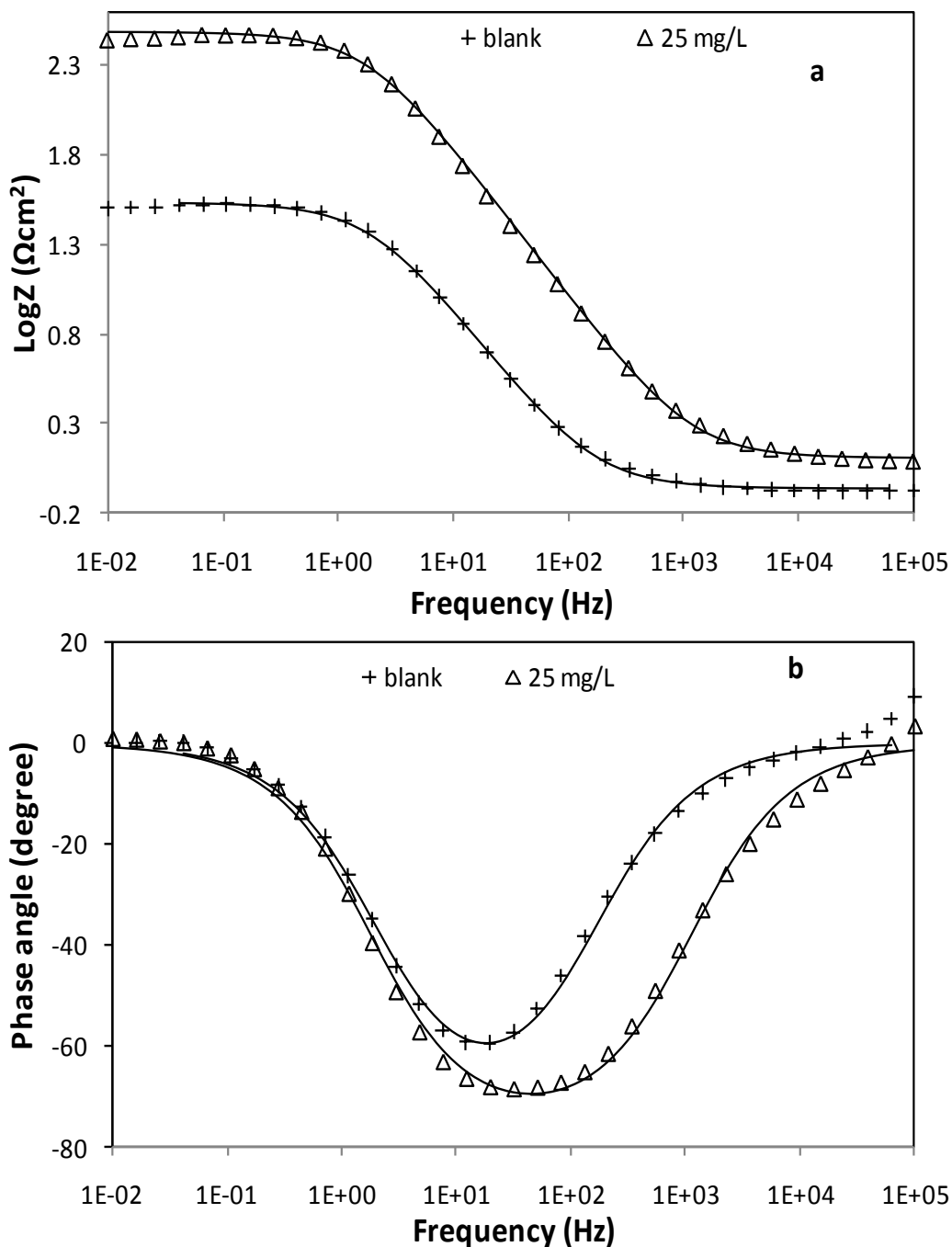**Figure 3.** Nyquist plots for C38 steel in 1 M HCl in the absence and presence of different concentrations of AEIC.

Figure 4. Bode plots, LogZ vs. freq (a) and phase angle vs. freq (b), for C38 steel in 1 M HCl in the absence and presence of 25 mg L^{-1} of AEIC.
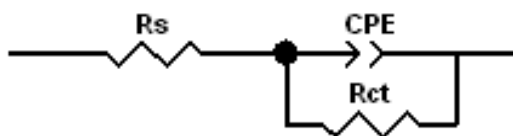

Figure 5. The equivalent circuit used to fit the impedance data, recorded for a C38 electrode 1 M HCl in the presence of different concentrations of AEIC.

Table 2. Values of the elements of equivalent circuit required for fitting the EIS for C38 steel in 1 M HCl in the absence and presence of different concentrations of AEIC and the corresponding inhibition efficiency.

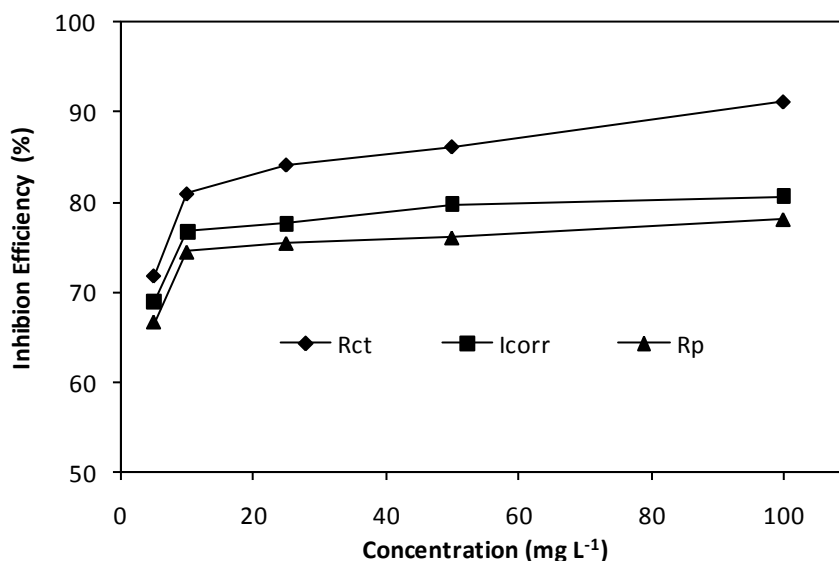| Concentration mg L^1	R_{ct}	10^4 A	n	C_{dl}	τ_d	IE
	(Ω cm^2)	(Ω^{-1} s^n cm^{-2})		(μF cm^{-2})	(s)	(%)
1 M HCl	49 ± 0.02	9.50 ± 0.73	0.853 ± 0.014	546	0.0268	—
AEIC						
5	174 ± 1.31	7.14 ± 0.24	0.841 ± 0.038	481	0.0838	72
10	257 ± 1.27	5.55 ± 0.16	0.862 ± 0.514	406	0.1044	81
25	309 ± 1.16	4.57 ± 0.80	0.878 ± 0.024	348	0.1076	84
50	354 ± 2.87	3.94 ± 0.52	0.886 ± 0.086	306	0.1082	86
100	553 ± 1.07	2.72 ± 0.27	0.887 ± 0.105	214	0.1182	91

Figure 6. Variation of inhibition efficiency, obtained from three methods, with extract concentration for C38 steel in 1 M HCl.

3.3. Effect of temperature

3.3.1. potentiodynamic polarization

The effect of temperature on the various corrosion parameters E_{corr}, I_{corr} and *IE* was studied in 1 M HCl at temperature range 25–55 °C in the absence and presence of 100 mg L^{-1} of AEIC (Figs. 7 and 8). Variation of temperature has almost no effect on the general shape of the polarization curves. The results were listed in Table 3. An inspection of Table 3 shown that, as the temperature increased, the values of E_{corr} shift in the negative direction, while the values of I_{corr} increase and *IE* decrease. This

behaviour reflects physical adsorption of AEIC on the steel surface. In order to calculate the activation parameters of the corrosion process, Arrhenius equation (4) and transition state equation (5) were used

$$I_{corr} = K \, exp(-\frac{E_a}{RT})$$ (4)

$$I_{corr} = \frac{RT}{Nh} exp(\frac{\Delta S_a}{R}) exp(-\frac{\Delta H_a}{RT})$$ (5)

where E_a is the apparent activation corrosion energy, T is the absolute temperature, k is the Arrhenius pre-exponential constant, R is the universal gas constant, h is Planck's constant, N is Avagadro's number, ΔS_a is the variation of entropy of activation and ΔH_a is the variation of enthalpy of activation. Fig. 9 show typical plots of log I_{corr} vs. $1/T$ for the uninhibited and inhibited solutions while Fig. 10 shows a representative plot for the transition state in 1 M HCl solutions without and with of 100 mg/L of AEIC. Activation parameters obtained from these graphs are given in Table 4. Inspection of Table 4 shows that values of both E_a and ΔH_a obtained in presence of AEIC are higher than those obtained in the inhibitor-free solutions. This observation further supports the proposed physical mechanism. Higher values of E_a suggests a physical adsorption mechanism [11-13], while unchanged or lower values of E_a in inhibited systems compared to the blank has been reported [31-33] to be indicative of chemisorption mechanism. On the other hand, the positive value of ΔH_a reflects the endothermic nature of the C38 steel dissolution process [34], while the increase of ΔS_a reveals that an increase in disordering takes place on going from reactant to the activated complex [35]. This behavior can be explained as a result of the replacement process of water molecules during adsorption of AEIC on steel surface. One can notice that E_a and ΔH_a values vary in the same way (Table 4).
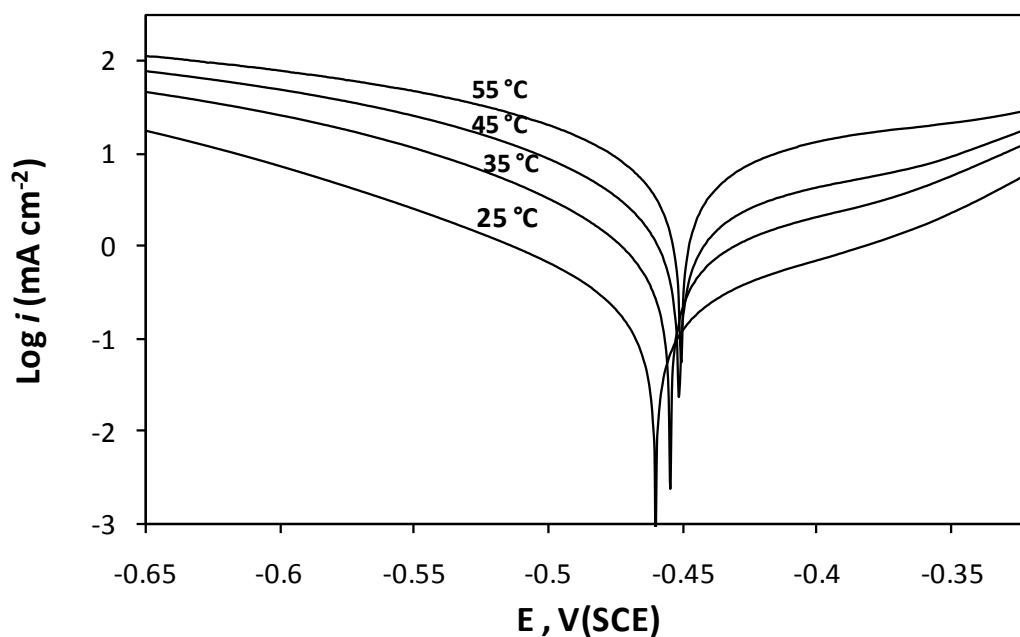

Figure 7. Effect of temperature on the cathodic and anodic responses for C38 steel in 1 M HCl.

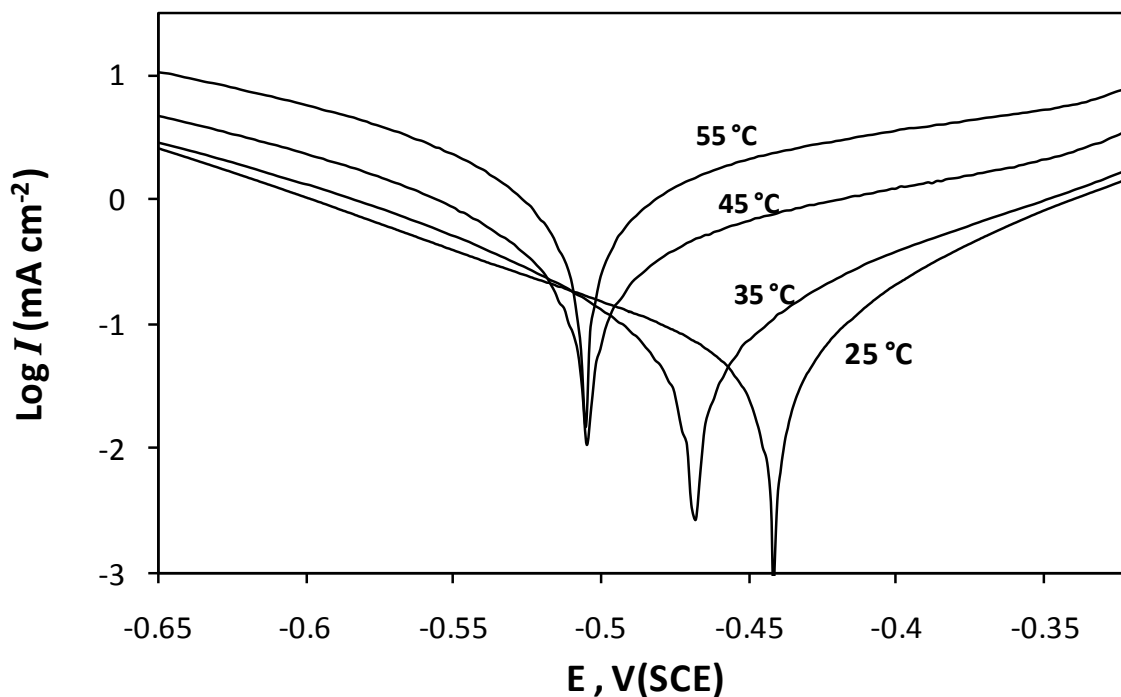**Figure 8.** Effect of temperature on the cathodic and anodic responses for C38 steel in 1 M HCl + 100 mg L^{-1} of AEIC.

Table 3. The influence of temperature on the electrochemical parameters for C38 steel electrode immersed in 1 M HCl and 1 M HCl + 100 mg L^{-1} of AEIC.

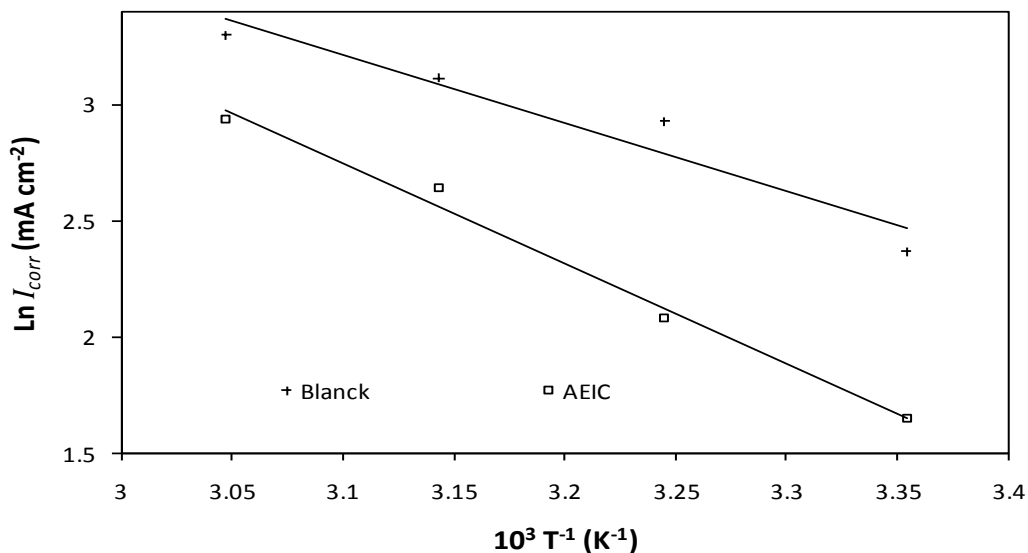| Temperature	E_{corr} vs SCE	I_{corr}	b_a	b_c	IE $_{Icorr}$
(°C)	(mV)	(µA cm^{-2})	(mV dec^{-1})	(mV dec^{-1})	(%)
1 M HCl					
25	-460	232	106	89	—
35	-454	843	111	109	—
45	-451	1192	120	109	—
55	-450	1982	131	116	—
100 mg L^{-1} of AEIC					
25	-443	45	122	78	81
35	-469	120	126	137	78
45	-505	434	135	162	64
55	-505	858	142	151	57

Figure 9. Arrhenius plots of corrosion ln I_{corr} vs. 1/T of 1 M HCl and 1 M HCl + 100 mg L^{-1} of AEIC.
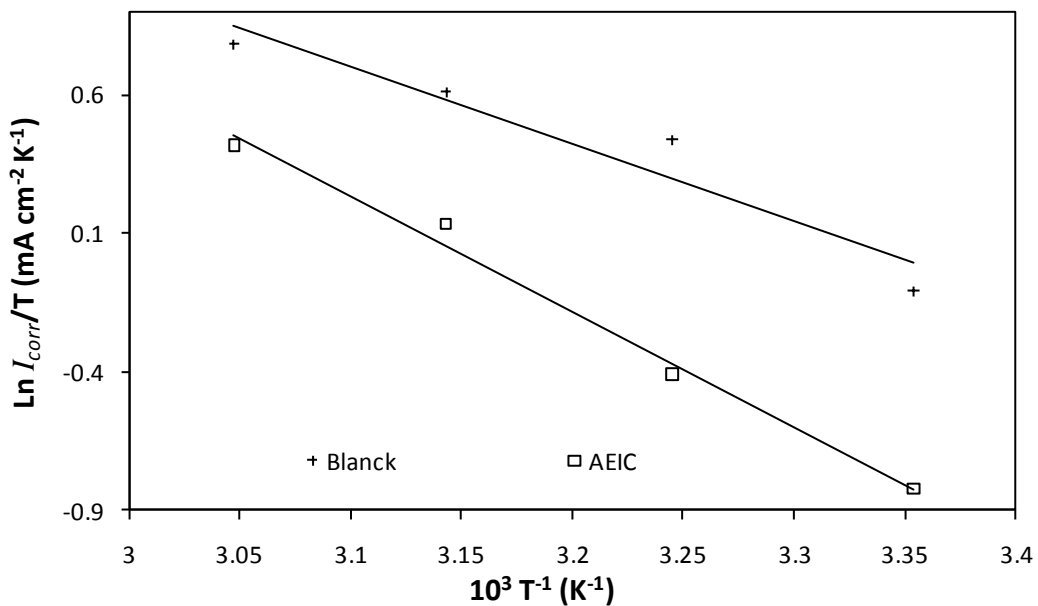

Figure 10. Arrhenius plots of corrosion ln (I_{corr} /T) vs. 1/T of 1 M HCl and 1 M HCl + 100 mg L^{-1} of AEIC.

Table 4. Thermodynamic parameters for the adsorption of AEIC in 1 M HCl on the C38 steel at different temperatures.

	E_a	ΔH_a	ΔS_a	E_a	ΔH_a	ΔS_a
	(kJ mol^{-1})	(kJ mol^{-1})	(J mol^{-1} K^{-1})	(kJ mol^{-1})	(kJ mol^{-1})	(J mol^{-1} K^{-1})
	From polarization curves			*From impedance measurements*		
1 M HCl	24.42	23.29	-119.48	28.00	26.87	-131.04
AEIC	35.78	34.70	-88.00	46.98	45.85	-76.13

3.3.2. Impedance measurements

The effect of solution temperature on the impedance behaviour of C38 steel in HCl solution without and with 100 mg/L of AEIC has been studied and the results are given in Figs. 11 and 12 respectively. In the inhibited solutions, variation of temperature has almost no effect on the general shape of the Nyquist diagrams. While in the uninhibited solutions, an inductive loop appeared at low-frequency values. The presence of the LF inductive loop may be attributed to the relaxation process obtained by adsorption species like Cl_{ads}^{-} and H_{ads}^{+} on the electrode surface [36–39]. The impedance parameters obtained in 1 M HCl solution are given in Table 5. These results were obtained from the previously proposed equivalent circuit in Fig. 5, while the EC shown in Fig. 13 was used for the impedance spectra containing one capacitive loop and an inductive loop. The results demonstrate that values of R_{ct} obtained in the uninhibited medium are decreased while those of C_{dl} are increased indicating the increase in the corrosion rate. The decrease in values of the CPE's exponent, n, with the rise of temperature is an indication for the increase of electrode surface roughness. In the inhibited solution, the same behaviour is observed. The decrease of n values with temperature reflects that the electrode surface becomes more heterogeneous as a result of desorption of AEIC. Values of IE% deduced from R_{ct} values are also included in Table 5 and it is clearly seen that the compound becomes less efficient at the highest temperature.
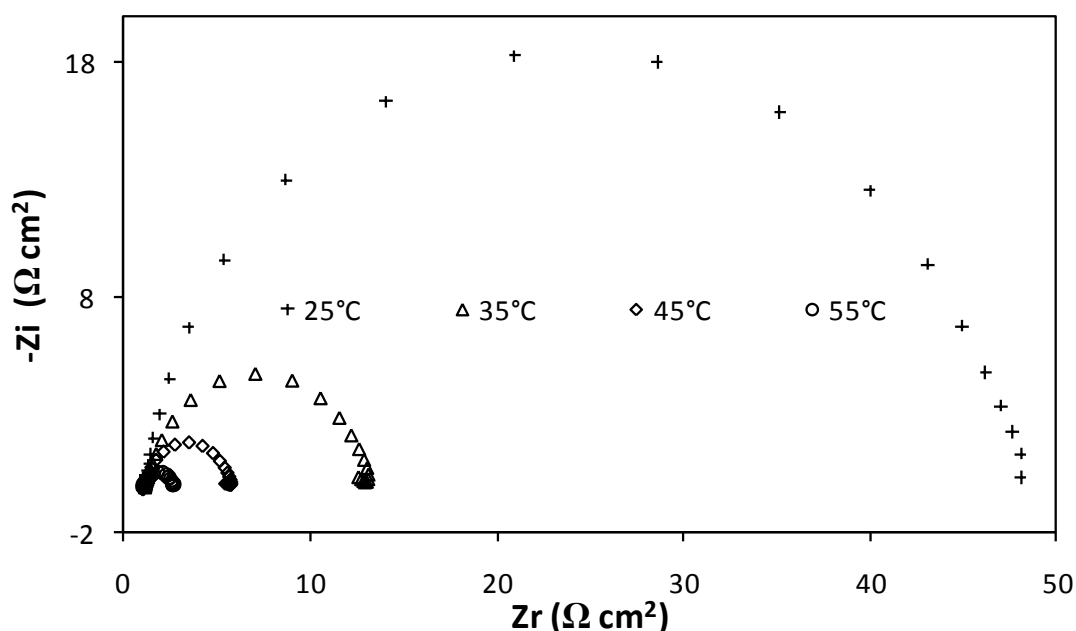

Figure 11. Nyquist diagrams for C38 steel in 1 M HCl at different temperatures.

To obtain the activation parameters from the impedance technique, values of R_{ct} and those of b_c and b_a obtained at different temperature were used to calculate values of I_{corr} according to Stern–Geary [40] equation.

$$I_{corr} = \frac{\beta_a \beta_c}{2.303(\beta_a + \beta_c)} \left(\frac{1}{R_{ct}} \right) \tag{6}$$

The activation parameters E_a, ΔH_a and ΔS_a are included in Table 4. The results are in good agreement with those obtained from polarization studies and show the same trend.
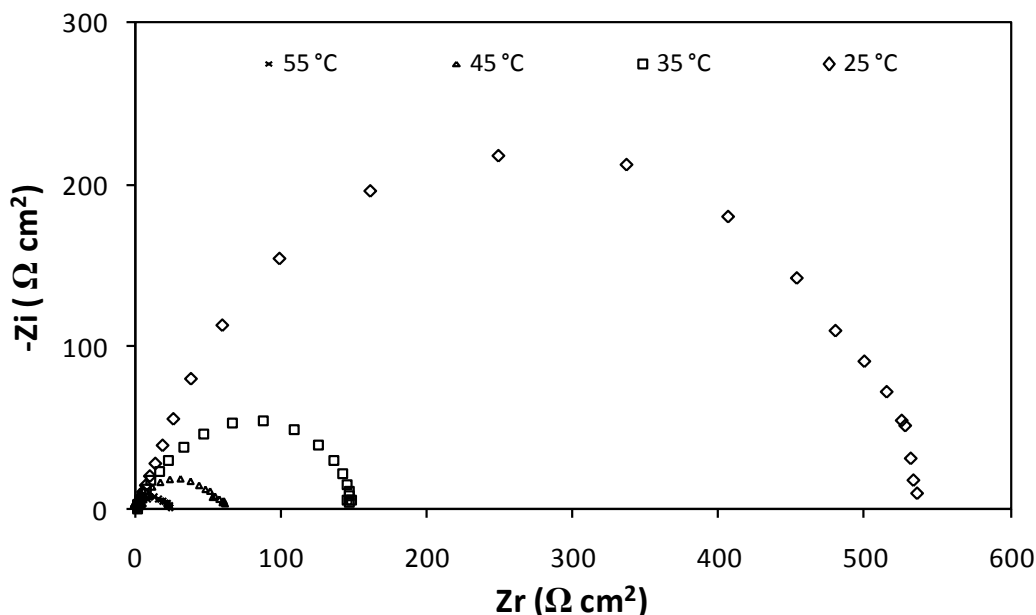

Figure 12. Nyquist diagrams for C38 steel in 1 M HCl + 100 mg L^{-1} of AEIC at different temperatures.
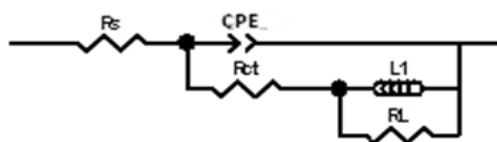

Figure 13. The equivalent circuit used to fit the impedance spectra containing one capacitive loop and an inductive loop.

3.4. Adsorption Isotherm

The values of surface coverage to different concentrations of inhibitors, obtained from Tafel extrapolation and impedance measurements at 25 °C, have been used to explain the best isotherm to determine the adsorption process. Adsorption isotherms are very important in determining the mechanism of organo-electrochemical reactions [41]. The most frequently used isotherms are

Langmiur, Temkin, Frumkin, Parsons, Hill de Boer, Flory–Huggins and Dahar–Flory–Huggins and Bockris– Swinkel [42–48]. All these isotherms are of the general form:

$$\smallint(\theta, x)\exp(2a\theta) = KC_{inh} \tag{7}$$

where $\smallint(\theta,x)$ is the configurational factor which depends upon the physical model and the assumptions underlying the derivation of the isotherm. "θ" is the surface coverage degree, "C" is the inhibitor concentration in the bulk of solution "a" is the lateral interaction term describing the molecular interactions in the adsorption layer and the heterogeneity of the surface. "K" is the adsorption–desorption equilibrium constant. The surface coverage θ for different concentrations of AEIC in 1 M HCl at 25 °C for 3 h of immersion time has been evaluated from impedance and polarization values.

Table 5. Values of the elements of equivalent circuit required for fitting the EIS for C38 steel immersed in 1 M HCl and 1 M HCl + 100 mg L^{-1} of AEIC at different temperatures.

Temperature	R_{ct}	C_{dl}	n	L	R_L	IE
(°C)	(Ω cm^2)	(μF cm^{-2})		(H cm^{-2})	(Ω cm^2)	(%)
1 M HCl						
25	49 ± 0.02	546	0.853 ± 0.014	—	—	—
35	17 ± 0.64	863	0.795 ± 0.421	18 ± 1.87	6 ± 1.26	—
45	12 ± 0.94	1583	0.745 ± 0.362	15 ± 2.35	3 ± 0.87	—
55	3 ± 0.96	1834	0.735 ± 0.093	10 ± 8.54	2 ± 1.25	—
AEIC						
25	553 ± 1.07	214	0.887 ± 0.105	—	—	91
35	160 ± 1.16	313	0.807 ± 0.103	—	—	86
45	67 ± 1.04	426	0.786 ± 0.054	—	—	78
55	14 ± 0.55	435	0.764 ± 0.073	—	—	75

Figs. 14, 15 and 16 represent fitting of impedance and polarization data obtained for C38 electrode in 1 M HCl containing various concentrations of AEIC to Langmuir, Temkin and Frunkin isotherms (Eqs. 8, 9 and 10).

$$\frac{C_{inh}}{\theta} = \frac{1}{K} + C_{inh} \qquad \text{(Langmuir isotherm)} \tag{8}$$

$$\left(\frac{\theta}{1-\theta}\right)\exp(-2a\theta) = KC_{inh} \qquad \text{(Frumkin isotherm)} \tag{9}$$

$$\exp(-2a\theta) = KC_{\text{inh}} \qquad \text{(Temkin isotherm)} \qquad (10)$$

The best correlation between the experimental results, obtained from the three tested isotherm functions was obtained using Langmuir adsorption isotherm. The values of correlation coefficient (R^2) were used to determine the best fit isotherm. Perfectly linear plots were obtained with correlation coefficient of (0.9993–1) using Langmuir adsorption isotherm.
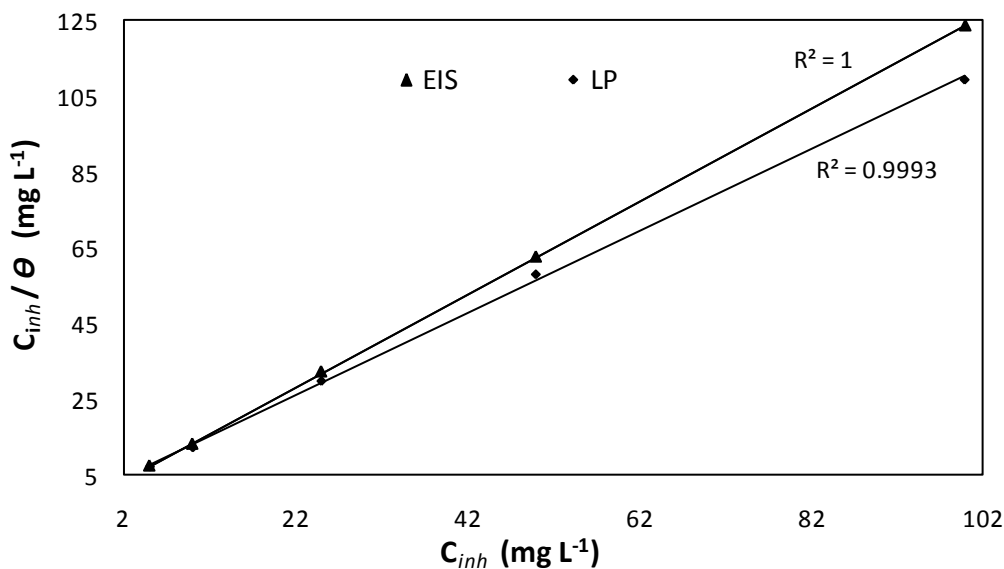

Figure 14. Langmuir adsorption plots for C38 steel in 1 M HCl containing different concentrations of AEIC.
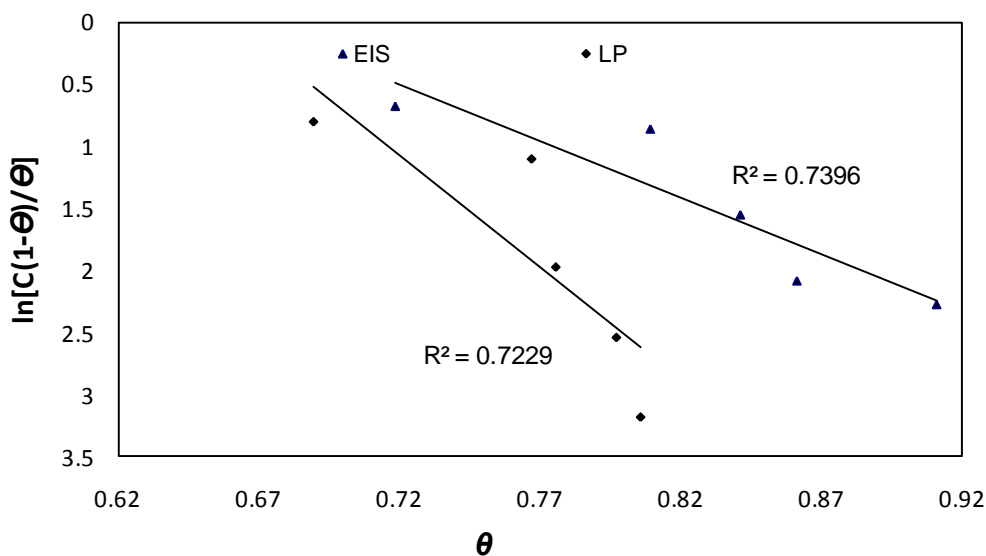

Figure 15. Frumkin adsorption plots for C38 steel in 1 M HCl containing different concentrations of AEIC.

The Langmuir isotherm is based on assumption that all adsorption sites are equivalent and that particle binding occurs independently from nearby sites being occupied or not [49]. It indicates that the adsorbing AEIC species occupies typical adsorption site at the metal/solution interface. As can be seen by the good fit, AEIC as inhibitor, found to follow Langmuir adsorption isotherm. It is very important to note that discussion of the adsorption behavior using natural product extracts as inhibitors in terms of thermodynamic parameters, such as the standard free energy of adsorption value (ΔG_{ads}) is not possible because the molecular mass of the extract components is not known. For example, there are a several alkaloid compounds in the extract. Some authors, in their study on acid corrosion with plant extract, noted the same limitation [12,13,16,17,19].
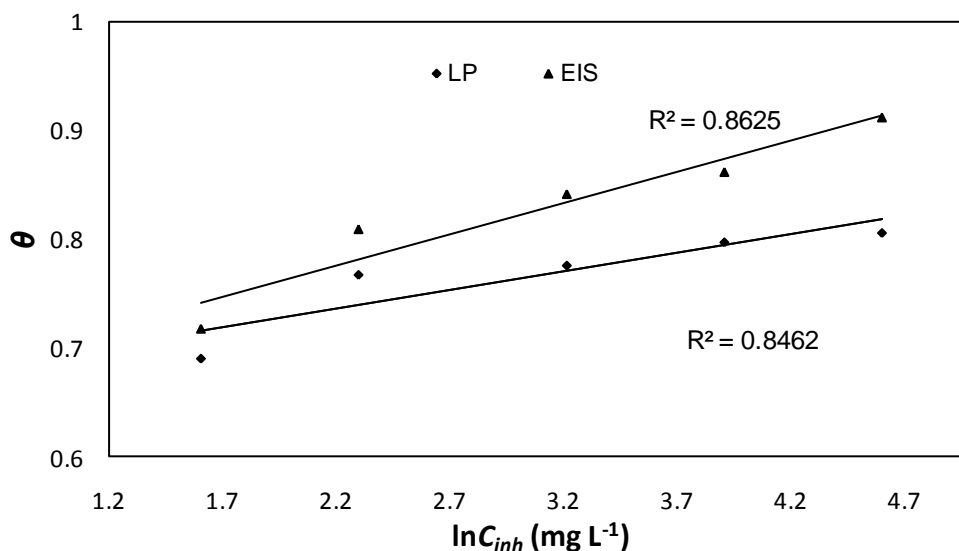

Figure 16. Temkin adsorption plots for C38 steel in 1 M HCl containing different concentrations of AEIC.

4. CONCLUSION

The present study shows that alkaloids extract from *Isertia coccinea* functioned as an inhibitor of C38 steel corrosion in hydrochloric acid media. Polarization measurements suggest a mixed-inhibition mechanism, which the impedance data indicate was achieved via adsorption of the extract species on the carbon steel surface. The protection efficiency of the extract, calculated from impedance and polarization measurements, was found to increase with increase in concentration of the inhibitor showing a maximum efficiency of 91 % at 100 mg L^{-1}. The effect of temperature on the electrochemical system shows that the extract becomes less efficient at the highest temperature. Adsorption models- Langmuir, Temkin and Frunkin isotherms were tested graphically for the data and the best fit was obtained with the Langmuir isotherm.

References

1. N.O. Eddy, E. E. Ebenso, *Int. J. Electrochem. Sci.* 5 (2010) 731.
2. N. Labjar, M. Lebrini, F. Bentiss, N. Chihib, S. El-Hajjaji, C. Jama, *Mater. Chem. Phys*. 119 (2010) 330.
3. B.M. Praveen, T.V. Venkatesha, *Int. J. Electrochem. Sci.* 4 (2009) 267.
4. M.G. Hosseini, M.R. Arshadi, *Int. J. Electrochem. Sci.* 4 (2009) 1339.
5. O.K. Abiola, J.O.E. Otaigbe*, Int. J. Electrochem. Sci.* 3 (2008) 191.
6. S.A.Abd El–Maksoud, *Int. J. Electrochem. Sci.* 3 (2008) 528.
7. M. Lebrini, F. Robert, H. Vezin, C. Roos, *Corros. Sci.* 52 (2010) 3367.
8. P.C. Okafor, E.E. Ebenso, U.J. Ekpe, *Int. J. Electrochem. Sci.* 5 (2010) 978.
9. I.B. Obot, N.O. Obi-Egbedi, S.A. Umoren, E.E. Ebenso, *Int. J. Electrochem. Sci.* 5 (2010) 994.
10. M. Dahmani, A. Et-Touhami, S.S. Al-Deyab, B. Hammouti, A. Bouyanzer, *Int. J. Electrochem. Sci.* 5 (2010) 1060.
11. M. Lebrini, F. Robert, C. Roos, *Int. J. Electrochem. Sci.* 5 (2010) 1698.
12. M. Lebrini, F. Robert, A. Lecante, C. Roos, *Corros. Sci.* 53 (2011) 687.
13. M. Lebrini, F. Robert, C. Roos, *Int. J. Electrochem. Sci.* 6 (2011) 847.
14. L. Vrsalovic, M. Kliškic, S. Gudic *Int. J. Electrochem. Sci.* 4 (2009) 1568.
15. I.B. Obot, N.O. Obi-Egbedi*, Int. J. Electrochem. Sci.* 4 (2009) 1277.
16. E.A. Noor, *Int. J. Electrochem. Sci.* 2 (2007) 996.
17. A.M. Abdel-Gaber, B.A. Abd-El-Nabey, M. Saadawy, *Corros. Sci*. 51 (2009) 1038.
18. J.C. da Rocha, J.A. da Cunha Ponciano Gomes, E. D'Elia, *Corros. Sci.* 52 (2010) 2341.
19. R. Kanojia, G. Singh, *Surf. Eng*. 21 (2005) 180.
20. A. Ostovari, S.M. Hoseinieh, M. Peikari, S.R. Shadizadeh, S.J. Hashemi, *Corros. Sci.* 51 (2009)1935.
21. P.C. Okafor, V.I. Osabor, E.E. Ebenso, *Pigm. Res. Technol.* 35 (2007) 299.
22. V.U. Khuzhaeu, S.F. Aripova, *Chem. Nat. Compd.* 36 (2000) 418.
23. A.U. Ogan, *Phytochem. Rep.* 99 (1971) 441.
24. P.C. Okafor, U.J. Ekpe, E.E. Ebenso, E.M. Umoren, K.E. Leizou, *Bull. Electrochem.* 21 (2005) 347.
25. A. Lecante, F. Robert, P.A. Blandinières, C. Roos, *Curr. Appl. Physics* 11 (2011) 714.
26. J. Bruneton, *pharmacognosie-phytochimie, plantes médicinales*, 4ème édition, revue et augmenté, Tec&Doc-Edition Médicinales Internationales Paris, 2009, 1288 p. (ISBN. 978-2-7430-1188-8).
27. S. Wu, Z. Cui, F. He, Z. Bai, S. Zhu, X. Yang, *Mater. Lett.* 58 (2004) 1076.
28. S. Martinez, M. Metikos-Hukovic, *J. Appl. Electrochem*. 33 (2003) 1137.
29. X. Wu, H. Ma, S. Chen, Z. Xu, A. Sui, *J. Electrochem. Soc.* 146 (1999) 1847.
30. H. Ma, X. Cheng, G. Li, S. Chen, Z. Quan, S. Zhao, L. Niu, *Corros. Sci.* 42 (2000) 1669.
31. G. Moretti, G. Quartaronr, A. Tassan, A. Zingales, Electrochim. Acta 41 (1996) 1971.
32. S. Martinez, I. Stern, J. Appl. Electrochem. 31 (2001) 973.
33. S.S. Abd El–Rehim, M.A.M. Ibrahim, K.F. Khaled, Mater. Chem. Phys. 70 (2001) 268.
34. N.M. Guan, L. Xueming, L. Fei, Mater. Chem. Phys. 86 (2004) 59.
35. S. Martinez, I. Stern, Appl. Surf. Sci. 199 (2002) 83.
36. M.A. Amin, S.S. Abd El-Rehim, E.E.F. El-Sherbini, R.S. Bayyomi, *Electrochim. Acta* 52 (2007) 3588.
37. H.J.W. Lenderrink, M.V.D. Linden, J.H.W. De Wit, *Electrochim. Acta* 38 (1993) 1989.
38. M. Kedam, O.R. Mattos, H. Takenouti, *J. Electrochem. Soc.* 128 (1981) 257.
39. M.A. Veloz, I. Gonzalez, *Electrochim. Acta* 48 (2002) 135.
40. M. Stern, A.L. Geary, *J. Electrochem. Soc.* 104 (1957) 56.

41. X. Wu, H. Ma, S. Chen, Z. Xu, A. Sui, *J. Electrochem. Soc.* 146 (1999) 1847.
42. I. Langmuir, *J. Am. Chem. Soc.* 39 (1917) 1848.
43. R. Alberty, R. Silbey, Physical Chemistry, second ed., Wiley, New York, 1997. p. 845.
44. J.O'M. Bockris, S.U.M. Khan, Surface Electrochemistry: A Molecular Level Approach, Plenum Press, New York, 1993.
45. J.W. Schapinik, M. Oudeman, K.W. Leu, J.N. Helle, *Trans. Farad. Soc.* 56 (1960) 415.
46. O. Ikeda, H. Jimbo, H. Tamura, *J. Electroanal. Chem.* 137 (1982) 127.
47. J. Hill de Boer, The Dynamical Character of Adsorption, second ed., Clarendon Press, Oxford, UK, 1986.
48. H. Dhar, B. Conway, K. Joshi, *Electrochim. Acta* 18 (1973) 789.
49. K.F. Khaled, N. Hackerman, *Electrochim. Acta* 48 (2003) 2715.